Inorganic Chemistry

Article

pubs.acs.org/IC

On the Intercalation of the Iodine–Iodide Couple on Layered Double Hydroxides with Different Particle Sizes

Maria Bastianini,[†,‡] Daniele Costenaro,[‡] Chiara Bisio,[‡,§] Leonardo Marchese,[‡] Umberto Costantino,[†] Riccardo Vivani,[†] and Morena Nocchetti[†,*]

[†]CEMIN "Centro di Eccellenza Materiali Innovativi Nanostrutturati" Dipartimento di Chimica, Università di Perugia Via Elce di Sotto 8, I-06123 Perugia Italy

[‡]DISTA "Centro interdisciplinare Nano-SiSTeMI" Dipartimento di Scienze e Tecnologie Avanzate, Università del Piemonte Orientale, via T. Michel 11, 1-15100 Alessandria, Italy

[§]ISTM-CRN Istituto di Scienze e Tecnologie Molecolari, via G. Venezian 21, Milano, Italy

Supporting Information

ABSTRACT: Molecular iodine was intercalated from non-aqueous solution into microsized ZnAl-layered double hydroxide (LDH) in the iodide form, generating the I_3^-/I^- redox couple into the interlayer region. Chloroform, ethanol, acetonitrile, or diethyl ether were used as solvents to dissolve the molecular iodine. The intercalation compounds were characterized by thermogravimetric analysis, X-ray powder diffraction, UV–vis spectroscopy, and scanning and transmission electron microscopy. The stability of iodine–solvent adducts and the iodine concentration affected the LDH iodine loading, and samples with I_2/I^- molar ratio ranging from 0.14 to 0.82 were prepared. Nanosized, well dispersible LDH, synthesized by the urea method in water–ethylene glycol media, were also prepared and successfully functionalized with the I_3^-/I^- redox couple applying the conditions optimized for the micrometric systems.

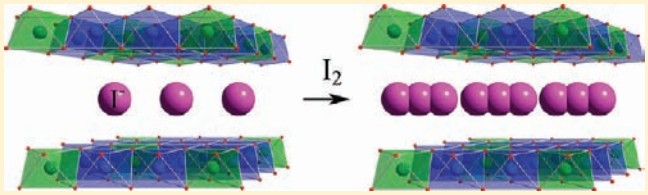

INTRODUCTION

The great challenge of this century is the finding of sustainable energy sources that can replace fossil fuels. Solar energy is one of the most promising renewable sources, and many chemical and physical methods are currently used for its harvesting. One of the most promising light to electricity conversion methods involves the use of the so-called "dye sensitized solar cells" (DSC),[1] due to their potential advantages of high efficiency energy conversion and low production cost. The working principle of a DSC device is based on ultrafast electron injection from a photoexcited dye into the conduction band of TiO_2 semiconductor and subsequent dye regeneration and hole transportation to the counter electrode.[2] Dye regeneration is attained by exploiting redox mediators like I_3^-/I^- redox couple contained in liquid phase electrolyte. Unfortunately, the liquid electrolyte presents several technological problems such as solvent evaporation, leakage of volatile solvent, and environmental toxicity. In the recent literature different studies have been devoted to the substitution of liquid electrolytes with organic hole transporting materials[3] and solvent-free polymer electrolytes incorporating triiodide/iodide as a redox couple.[4] Some papers in the literature also proposed the use of solid-state electrolytes (i.e., CuI, CuBr, CuSCN, CuI/molten salts composite materials).[5] Nevertheless, the use of these materials presented some disadvantages such as low light-to-electricity conversion efficiency due to low ionic conductivity and poor electrolyte/photoelectrode interfacial contact.[6] To limit this problem, attention was focused on quasi-solid-state electrolytes prepared by incorporating inorganic additives (i.e., natural clays, silica particles, etc.) to classical solvent or ionic liquids aiming to reduce solvent evaporation and improve electrode–electrolyte interfacial contact.[7]

The use of gels or quasi-solid electrolytes may largely simplify the DSC design and produce a significant improvement in energy-conversion efficiency and long-term stability.[8] In this connection, the development of suitable low dimensional inorganic compounds able to host the I_3^-/I^- couple and to form dispersed systems is of great interest.

Among 2D compounds, layered double hydroxides (LDH) are promising materials in a wide range of application because of their broad possibility of manipulation to obtain functional materials. As a matter of fact, in these last two decades there has been a rapid growth in the number of scientific papers and industrial patents on LDH. In detail, LDH is represented by the general formula $[M(II)_{1-x}M(III)_x(OH)_2][A_{x/n}\cdot mH_2O]$, where M(III) cations are typically Al, Cr, Fe, or Ga and M(II) can be Mg, Zn, Ni, Co, or Cu. A is an exchangeable anion of ionic valence n, and x is the M(III)/(M(II) + M(III)) molar ratio. The x value generally ranges between 0.2 to 0.4 and determines the positive layer charge density and the ion exchange capacity (IEC) of the material.[9] The insertion, via ion exchange

Received: November 22, 2011
Published: February 8, 2012

   dx.doi.org/10.1021/ic202520v | *Inorg. Chem.* 2012, 51, 2560–2568

reactions, of selected inorganic or organic anions allows materials to be obtained for new stimulating applications in the fields of polymeric nanocomposites,[10] heterogeneous catalysis,[11] and photochemistry[12] and recently in field of photocatalysis.[13] Moreover, new strategies have been achieved to exfoliate LDH in two-dimensional nanosheets in order to obtain ordered thin films[14] especially for optical devices.[15] New materials can be designed and developed by the insertion of neutral molecules between the LDH sheets. Rare examples of intercalation reactions have been reported and concern the insertion of long-chain alkanols into the interlayer regions of LDH containing surfactants[16] or alkoxides.[17]

An exciting challenge is to exploit the excellent intercalation properties of LDH materials immobilizing into the interlayer region the I_3^-/I^- redox couple, in different molar ratios, to obtain a quasi-solid electrolyte for DSC devices. A number of detailed studies on the preparation and characterization of iodide and, in general, of halides containing LDH have been conducted,[18] while to the best of our knowledge, only two works report on the intercalation of triiodide. Mohanambe and Vasudevan[19] aimed to extend the host−guest LDH chemistry to the inclusion of inorganic nonpolar molecules as molecular iodine by intercalation of carboxymethyl-β-cyclodextrins (CDs), which retained their accessible cavities and ability to complex iodine molecules. Recently, Ma et al.[20] used an innovative redox intercalation reaction to prepare non-Al^{3+}-based LDH having iodide and triiodide as counterions. In particular, CoFe-LDH was synthesized contacting brucite-like $Co(II)_{1-x}Fe_x(II)(OH)_2$ with a solution of iodine in chloroform. The iodine acted as oxidizing agent of Fe^{2+} to Fe^{3+}, generating an excess of positive charges on the lamellae, and the electroneutrality of the solid was maintained by iodide intercalation. Intercalation of triiodide was also observed using concentrated iodine solutions.

The present work reports a study on the intercalation of the triiodide/iodide redox couple in the interlayer region of micro- and nanosized LDH. The ion-exchange between ZnAl-LDH interlayer anions with triiodide anions and the intercalation of I_2 from nonaqueous solution into ZnAl-LDH in the iodide form have been investigated. It has been found that the solvent nature and the iodine concentration play a key role to obtain materials with tunable triiodide/iodide molar ratio. Well dispersible I_3^-/I^- containing LDH having nanometric dimensions was prepared, modifying the synthesis procedure and using water and ethylene glycol as solvent.[21] As an unexpected and very interesting result, this method yielded, directly from the synthesis, nanometric LDH compounds in anionic forms different from carbonate, depending on the metal salt used for its synthesis.

EXPERIMENTAL SECTION

Materials. All the chemicals used in this work were C. Erba RP-ACS products.

Synthesis of Microsized ZnAl-I_2. The LDH $[Zn_{0.61}Al_{0.39}(OH)_2](CO_3)_{0.195}\cdot 0.5H_2O$ (hereafter ZnAl-CO_3) was synthesized using the urea method.[17] The chloride form (hereafter named ZnAl−Cl) with formula $[Zn_{0.61}Al_{0.39}(OH)_2](Cl)_{0.39}\cdot 0.6H_2O$ was obtained by titrating the carbonate form, dispersed in a 0.1 M NaCl solution, with a 0.1 M HCl by means of a Radiometer automatic titrator operating at pH stat mode and pH value of 5. The ZnAl-Cl was equilibrated with a 1 M potassium iodide solution (1 g LDH/35 mL KI) under magnetic stirring for 1 day, using CO_2-free and deionized water and working under nitrogen atmosphere. The resulting compound, with formula $[Zn_{0.61}Al_{0.39}(OH)_2](Cl)_{0.17}I_{0.22}\cdot 0.34H_2O$ (hereafter named ZnAl-I), was washed two times with deionized water and dried at room temperature.

ZnAl-I was equilibrated with 0.1 and 0.5 M of I_2 solution in different organic solvents: ethanol, diethyl ether, chloroform, or acetonitrile (1 g LDH/13 mL I_2 solution), under magnetic stirring for 3 days. The obtained solids were recovered by centrifugation, washed with the solvent used for the intercalation, and dried at room temperature. The obtained materials with maximum I_2 content (using 0.5 M solutions) were labeled as ZnAl-I_2solv, where solv indicates the solvent used for the intercalation: cf (chloroform), et (ethanol), ac (acetonitrile), or de (diethylether).

Synthesis of Nanosized ZnAl-I_2. Nanosized LDH containing chloride anions (hereafter named *n*-ZnAl-Cl) in the interlayer region have been synthesized adapting the urea method.[17] A total of 500 mL of 1 M solution of Zn(II) and Al(III) having molar fraction Al(III)/(Al(III) + Zn(II)) equal to 0.30 was prepared dissolving 85.5 g (350 mmol) of $ZnCl_2\cdot 6H_2O$ and 36 g (150 mmol) of $AlCl_3\cdot 6H_2O$ in a water−ethylene glycol 1:2 (v/v) mixture. A total of 36 g (600 mmol) of solid urea were then added to this solution so that the urea/Al molar ratio was 4. The clear solutions were heated, under stirring, at reflux temperature for 6 h. The gelatinous materials obtained were recovered by centrifugation and washed two times with water. Finally, the materials were stored as colloidal dispersions in 300 mL of water and ethylene glycol [1:2 (v/v)]. In order to determine the solid amount per volume unit, a known volume of dispersion was washed two times with distilled water to remove the ethylene glycol and dried in an oven at 80 °C. The dispersion contained 165 mg of *n*-ZnAl/mL of dispersion.

A total of 6 mL of *n*-ZnAl-Cl dispersion was washed two times with deionized water and exchanged with iodide using the conditions described for the microsized LDH. The obtained *n*-ZnAl-I was then contacted with 10 mL of 0.5 M I_2 solution in acetonitrile in order to generate triiodide in the interlayer region.

Characterization. The Zn and Al content of the solid was determined by Inductively Coupled Plasma-Optical Emission Spectrometer (ICP-OES) Varian 700-ES series after dissolving the samples in concentrated HNO_3 and properly diluting them.

Iodide content was determined by ion-chromatography (IC): complete I^- and I_3^- deintercalation was achieved by equilibrating ∼100 mg of sample in 20 mL of 1 M Na_2CO_3 solution for 12 h. The surnatant solution was then analyzed with a Dionex 2000 ion chromatographer.

The X-ray powder diffraction (XRPD) patterns were taken with a Philips X'PERT PRO MPD diffractometer operating at 40 kV and 40 mA, step size 0.0170 2θ degrees, and step scan 20 s, using the Cu Kα radiation and an X'Celerator detector.

Rietveld refinement of ZnAl-I was performed using the GSAS program.[22]

Water and carbonate content of the solids were determined by coupled thermogravimetric (TG) and differential thermal (DTA) analyses performed with a Netzsch STA 449C apparatus, in air flow and heating rate of 10 °C/min. This technique allowed chloride, iodide, and triiodide content to also be checked.

Diffuse reflectance UV−vis (DR UV−vis) spectra were recorded using a Perkin-Elmer Lambda 900 spectrometer. Measurements on powder samples were collected by using a diffuse reflectance sphere accessory. Before the analysis, the samples were dispersed in anhydrous $BaSO_4$ (10 wt %).

The morphology of the LDH particles was investigated with a Philips 208 transmission electron microscope (TEM). A small drop of the dispersion of LDH in ethanol was deposited on a copper grid precoated with a Formvar film and then evaporated in air at room temperature.

Fourier transform infrared spectra (FT-IR) of different samples, dispersed in KBr pellets, were recorded at rt using a Bruker Tensor 27 spectrometer. Typically, each spectrum was obtained averaging over 50 scans at a resolution of 2 cm^{-1}.

Scanning electron microscope (SEM) images were acquired by a LEO 1450 VP; the samples were coated with a thin gold layer to ensure surface conductivity.

dx.doi.org/10.1021/ic202520v | Inorg. Chem. 2012, 51, 2560−2568

RESULTS AND DISCUSSION

For reader convenience, it seems useful to briefly recall the main structural features of layered double hydroxides. Figure 1

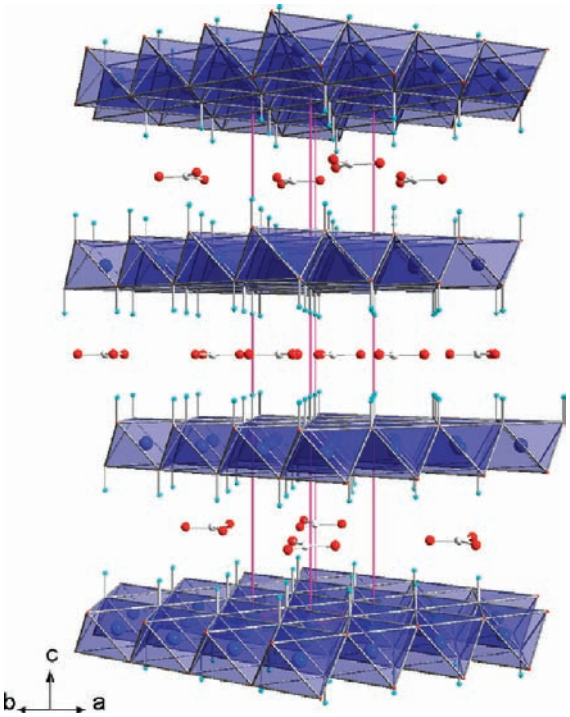

Figure 1. Schematic illustration of the LDH structure.

shows the sequence of four layers of the ZnAl-LDH. Each layer arises from the packing of layers built up of $M(OH)_6$ (M = Zn^{2+}, Al^{3+}) octahedral units with shared edges. In an ideal arrangement, $Al(OH)_6$ octahedral units are 33% of the total, and the Zn/Al atomic ratio is 2. The Al cations bear net positive charges balanced by anions located in the interlayer region.

The aim of this work is to insert the triiodide/iodide couple, in different molar ratios, in the constrained environment of the interlayer region of LDH to provide new redox properties. Two methods were tested; the first involved an ion-exchange of LDH interlayer anions with triiodide anions present in solution, while the other one consisted in an intercalation reaction of I_2 into LDH previously exchanged with I^- anions in order to form triiodide species in situ. The former method was pursued by contacting ZnAl-Cl samples with solutions of I_3^- in water or organic solvents as acetonitrile, chloroform, and ethanol. Despite several attempts and changing the I_3^- concentration, temperature, and reaction time, the direct I_3^- ion-exchange failed. The reasons for this were not deeply investigated; very likely it depended on the low charge density and on the large dimensions of the guest species that made the process thermodynamically unfavorable. On the contrary, the latter method gave satisfactory results. In the following the experimental data obtained through the I_2 intercalation in micro- and in nanosized LDH in the iodide form will be separately discussed.

Intercalation of the Triiodide/Iodide Redox Couple on Micrometric LDH. The XRPD patterns of LDH in carbonate, chloride, and iodide forms are compared in Figure 2. The first intense 003 peaks, related to the LDH metal atomic planes,

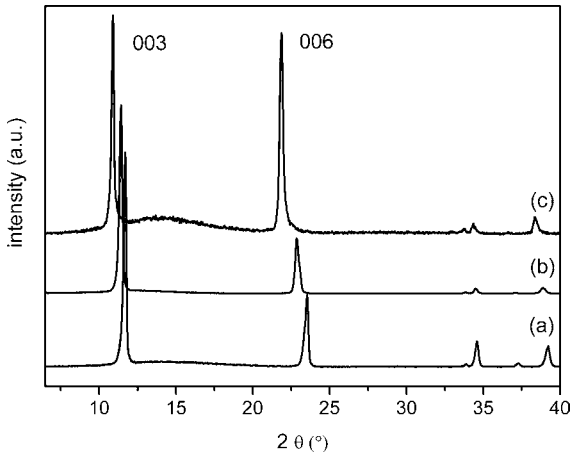

Figure 2. XRPD patterns of microsized ZnAl-CO_3 (a); ZnAl-Cl (b); and ZnAl-I (c).

indicate that the interlayer distances of ZnAl-CO_3 (7.56 Å), ZnAl-Cl (7.74 Å), and ZnAl-I (8.10 Å) increase in agreement with the increased anion dimensions. It is noteworthy that the relative intensity of the 006 reflection in the ZnAl-I pattern is higher than in other anionic forms, and this is related to the increase in electron density of the interlayer region, due to the presence of heavy iodine atoms arranged halfway between adjacent brucitic sheets.[23,20]

The composition of ZnAl-I indicates that a pure hydrotalcite phase in iodide form was not obtained, very likely because LDH has a poor affinity for I^- ions that prevented the complete I^-/Cl^- exchange. However, XRPD patterns showed the presence of only one phase, suggesting that iodide and chloride ions were randomly distributed in the interlayer region. The ZnAl-I crystal structure was therefore refined using the Rietveld method by placing Cl and I atoms in the same 18*h* crystallographic site and setting their occupancy values in order to fit the experimentally determined composition. The agreement was good, confirming our assumptions. Figure 3

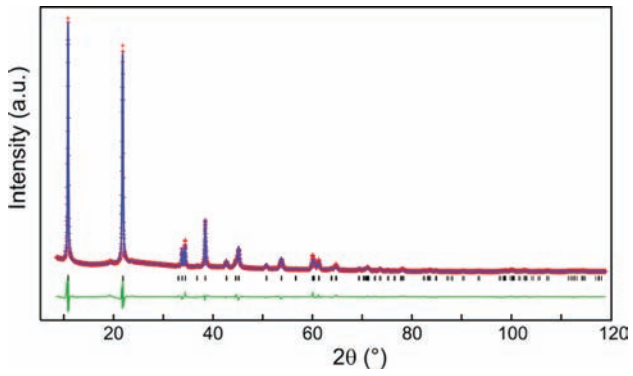

Figure 3. Experimental (+), calculated (−), and difference (bottom) profiles for $[Zn_{0.61}Al_{0.39}(OH)_2](Cl)_{0.17}I_{0.22}\cdot 0.34H_2O$.

shows the Rietveld plot of the last refinement cycle, while Table 1 reports on the refined crystal data and refinement details. (More details are given the Tables S1 and S2 of the Supporting Information.)

The intercalation of molecular iodine into ZnAl-I was carried out by contacting the ZnAl-I with 0.1 and 0.5 M I_2 solutions, using chloroform, ethanol, acetonitrile, and diethyl ether as solvents. These solvents were selected because of their ability to

dx.doi.org/10.1021/ic202520v | Inorg. Chem. 2012, 51, 2560−2568

Table 1. Crystal Data and Refinement Details for ZnAl-I

empirical formula	$Zn_{0.61}Al_{0.39}(OH)_2Cl_{0.17}I_{0.22}\cdot 0.34H_2O$
formula weight	124.51
crystal system	trigonal
space group	$R\bar{3}m$
a, Å	3.0807(1)
b, Å	3.0807(1)
c, Å	24.3941(4)
α, deg	90
β, deg	90
γ, deg	120
V, Å^3	200.50(1)
Z	3
calcd density, g cm^{-3}	3.10
wavelength, Å	1.54056
pattern range, 2θ/deg	8.5−120
step scan increment, 2θ/deg	0.017
time per step, s	60
no. of data points	6559
no. of reflections	112
no. of parameters	42
R_p	0.046
R_{wp}	0.067
R_F2	0.103
GOF	3.84

dissolve molecular iodine[24] and to interact with the hydrophilic LDH. The solids obtained turned their color from white to dark brown, indicating the presence of iodine. UV−vis spectroscopy (that will be discussed later on) showed that triiodide and higher polyiodide forms were present in the interlayer region, assessing that they were generated in situ by reaction of I_2 with the already intercalated iodide. However, for the sake of simplicity, the global iodine content of these samples will be considered in the following as I_2. Figure 4 shows the XRPD

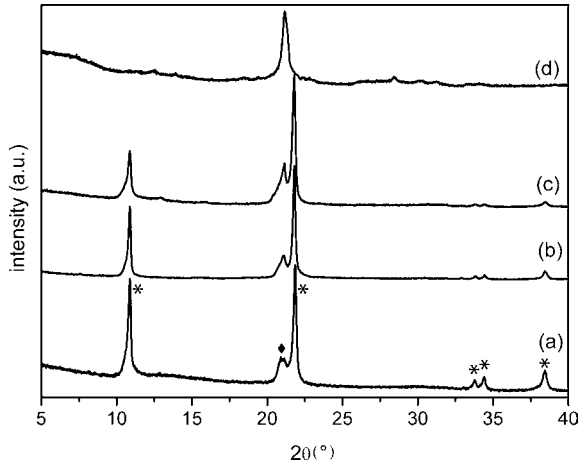

Figure 4. XRPD pattern of ZnAl-I_2de (a), ZnAl-I_2et (b), ZnAl-I_2cf (c), and ZnAl-I_2ac (d). * phase *a*, ♦ phase *b* (see text).

patterns of the samples obtained using 0.5 M I_2 solutions. In ZnAl-I_2de, ZnAl-I_2et, and ZnAl-I_2cf, the relative intensity of the 006 peak, at 4.05 Å, is increased and becomes higher than the 003 reflection, according to the increase of electron density of the interlayer region, due to iodine intercalation. This phase, with an increased amount of iodine in the interlayer region but the same interlayer distance, was indicated as phase *a*. Moreover, a new, intense diffraction peak at d = 4.22 Å that was attributed to the formation of a ZnAl-I_2 phase richer in iodine, with an interlayer distance of about 8.44 Å, appeared in all the patterns and was indicated as phase *b*. Phase *a* is completely converted into phase *b* in the sample ZnAl-I_2ac (Figure 4d). In this phase, due to the small interlayer distance, triiodide moieties should be intercalated with their main molecular axis parallel to brucitic layers. As a support of this hypothesis we have simulated the XRPD pattern (Figure 5) of

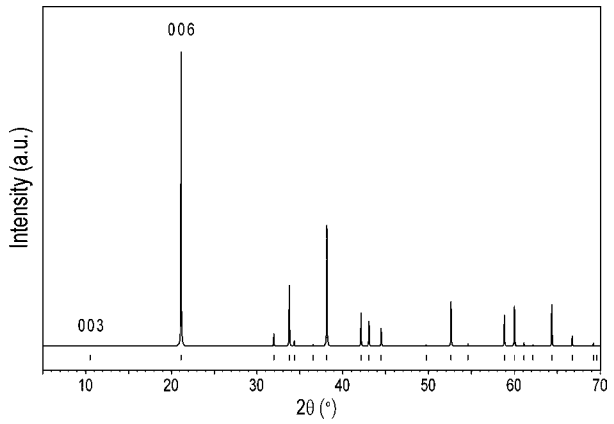

Figure 5. Simulated XRPD pattern of $Zn_{0.61}Al_{0.39}(OH)_2Cl_{0.17}I_{0.22}(I_2)_{0.18}\cdot 0.32H_2O$.

an LDH phase with composition similar to that experimentally observed in ZnAl-I_2ac: $Zn_{0.61}Al_{0.39}(OH)_2Cl_{0.17}I_{0.22}(I_2)_{0.18}\cdot 0.32H_2O$. It was assumed to be isostructural to ZnAl-I and with the following unit cell: a = 3.807 Å, c = 25.32 Å, which is an interlayer distance of $c/3$ = 8.44 Å. In this simulation, performed with the Powdercell program,[25] the total iodine content was taken into account by simply increasing the occupancy factor of the I atom in the interlayer region. Although approximated, the simulation shows that, due to the fact that the electron density of 003 metal hydroxide planes is close to that of the 006 interlayer planes, the former diffraction effect is virtually extinct, and only the 006 reflection at 4.22 Å is observed, as experimentally found.

The morphology of ZnAl-I_2 samples was investigated by SEM analysis (Figure S1 in Supporting Information). The micrographs shows hexagonal platelets having a diameter of about 10 μm.

The I_2 content was determined by TG analysis according to ref 26 and assuming that iodide and chloride contents remained unchanged during the intercalation process. The thermal behavior of ZnAl-I_2solv samples was interpreted on the basis of the TG curve of CsI_3. This salt loses 1 mol of I_2 in the 150−350 °C range. As an example, Figure 6A reports on a comparison between TG curves of ZnAl-I_2ac and CsI_3. Three steps of endothermic weight losses (DTA not shown) are evident in ZnAl-I_2ac, and the TG curve can be discussed as follows: (a) the first step, ranging from 80 to 180 °C, is due to the loss of the hydration water; (b) the second region, until 300 °C, corresponds both to the weight loss due to the dehydroxylation of the brucite layers and to the loss of iodine; and (c) the last step from 400 to 500 °C is relative to the loss of chloride and iodide anions as hydrogen chloride and iodide. The TG curves of all samples intercalated with 0.5 M solutions of I_2 in different solvents are reported in Figure 6B. As a general feature, all intercalated samples showed similar thermal

dx.doi.org/10.1021/ic202520v | Inorg. Chem. 2012, 51, 2560−2568

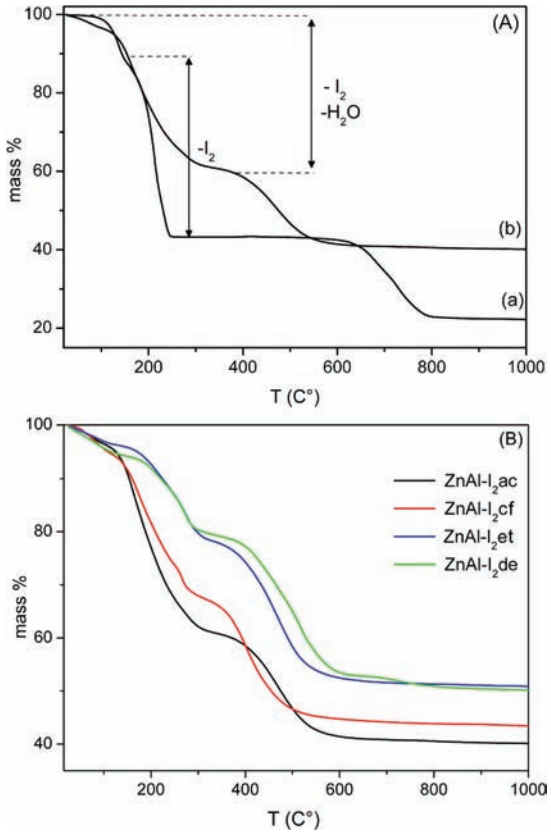

Figure 6. (A) TG curves of CsI_3 (a) and ZnAl-I_2ac (b); (B) TG curves of ZnAl-I_2solv samples.

behavior. Nevertheless, significant variation of weight losses in the 100−300 °C range are observed depending on the solvent used for the intercalation (Figure S2 of Supporting Information). However, FT-IR spectroscopic studies revealed that the samples did not contain any trace of solvent different from water, and therefore, the change in weight loss in that temperature range was ascribed to different I_2 contents.

Table 2. Composition of the ZnAl-I_2solv Samples[a]

	$[Zn_{0.61}Al_{0.39}(OH)_2]Cl_{0.17}I_{0.22}(I_2)_x \cdot nH_2O$		
sample	x	n	I_2/I^- molar ratio (%)
ZnAl-I_2de	0.030	0.22	13.6
ZnAl-I_2et	0.05	0.27	22.7
ZnAl-I_2cf	0.10	0.47	45.5
ZnAl-I_2ac	0.18	0.32	81.8

[a]The iodine uptake percentage, calculated referring to the iodide, is also reported.

Table 2 shows the composition of the materials obtained and the percentage of iodine intercalated referring to the iodide ($[I_2/I^-]$ molar ratio).

It is evident that the solvent (L) plays a key role in the final amount of the intercalated iodine. It can be justified on the basis of solvent−iodine interactions. It is indeed known that iodine forms adducts (L → I_2) with solvents having electron donor properties and that the stability of these adducts depends on the electron donor strength of the solvent as a Lewis base. The strength of the n-donor solvents, used in this work, increases in the following order: chloroform ≪ ethanol < acetonitrile < diethyl ether.[27] During the intercalation process, the solvation sphere of molecular iodine is modified, passing from organic molecules to water. The enthalpy associated to this process is positive, which is unfavorable to the molecular iodine intercalation, and increases with the stability of the L → I_2 complex. The low iodine loading obtained from diethyl ether and ethanol is in agreement with the above considerations. An increase of iodine uptake was observed with chloroform, which is a noncoordinating solvent.

The best results, in terms of iodine uptake percentage, were obtained using acetonitrile as solvent, reaching 81.8%. This behavior cannot be explained with the above considerations, because acetonitrile is a good coordinating and very polar solvent, and very likely, in this case a different intercalation mechanism may take place. UV−vis spectra of the diluted equilibrating solutions (10^{-6} M) were collected in order to indentify the iodine species present in the different solvents (Figure 7). UV−vis spectra of I_2 in ethanol and diethyl ether

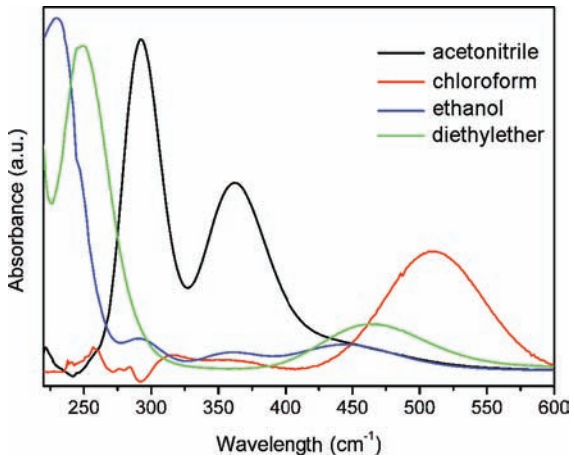

Figure 7. UV−vis spectra of 10^{-6} M I_2 solutions in the indicated solvents.

show two bands due to molecular I_2 (centered at 446 and 465 nm for ethanol and diethyl ether, respectively) and to the L → I_2 charge transfer complex (centered at 230 and 250 nm for ethanol and diethyl ether, respectively). In these solvents, both free molecular and complexed iodine are present. On the contrary, the UV−vis spectrum of I_2 in chloroform shows only the molecular iodine band centered at 510 nm, indicating that all the iodine is free and available to the intercalation. Finally, in the spectrum of I_2 in acetonitrile the absorption bands associated to iodine are not present, while there are two bands at 292 and 362 nm, typical of triiodide, indicating the presence of this anion in solution.[28] Triiodide anions are produced by a sequence of reactions in which a slow transition of the outer complex (L → I_2) to the inner complex (L → I^+I^-) occurs. The inner complex produces iodide that can bind molecular iodine, forming triiodide anions.[29] These results should be explained considering the ability of this solvent to stabilize the ionic species due to its high dielectric constant.

From these considerations we may conclude that in chloroform the intercalation reaction very likely mainly involves molecular iodine, while in acetonitrile, besides the intercalation of molecular iodine, the ion exchange of I_3^- with I^- occurs. Considering the selectivity scale for the halides F^- > Cl^- > Br^-

dx.doi.org/10.1021/ic202520v | Inorg. Chem. 2012, 51, 2560−2568

> I^-,[30] it is reasonable to assume that iodide is exchanged preferentially over chloride. Chemical analysis indicated that the chloride content of samples before and after the intercalation reactions was the same, confirming this assumption. Also, the I_2 concentration in the equilibrating solution strongly affects the amount of the intercalated iodine. Intercalation reactions carried out with 0.1 M I_2 solutions generally led to a lower amount of intercalated iodine for all solvents, as shown by comparing the data reported in Table 2 and Table S3 of Supporting Information.

DR-UV−vis reflectance spectra of intercalated samples are reported in Figure 8. Two intense bands at about 290 and 370

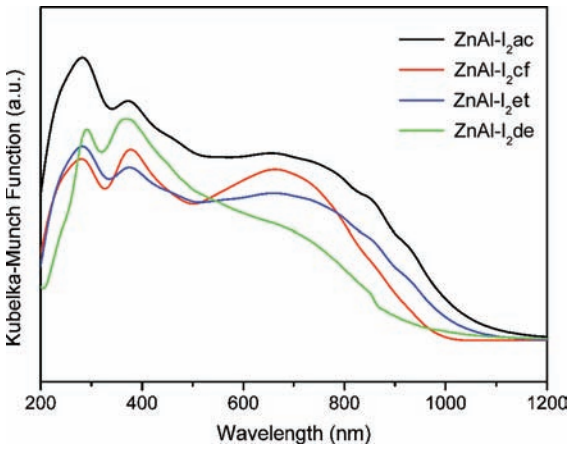

Figure 8. DR-UV−vis spectra of ZnAl-I_2solv samples.

nm (Figure 8), corresponding respectively to the spin- and symmetry-allowed $\sigma \rightarrow \sigma^*$ and $\pi \rightarrow \sigma^*$ transitions of the linear I_3^- species, have been detected for all samples thus indicating that the intercalation procedure results in the formation of I_3^- species.[24,31] Moreover, an evident shoulder at 230 nm, assigned to I^-, is especially observed for samples intercalated by using ethanol, chloroform, and diethylether. The large absorption in the 500−1000 nm range, having a maximum ranging from 600 to 750 nm, can be assigned to the formation of the pentaiodide ions.[19] From the obtained data it is also possible to observe that the use of acetonitrile as solvent for intercalation (sample ZnAl-I_2ac) promotes the formation of a higher amount of polyiodide species, which are probably stabilized by the host−guest interactions. Recently, iodine was efficiently loaded in porous organic cages via vapor sublimation.[32] Also in this case, the host structure was recognize to stabilize iodine as I_5^-.

Intercalation of the Triiodide/Iodide Redox Couple on Nanometric LDH. As underlined in the introduction, materials containing the triiodide/iodide redox couple can be used to produce gel- or quasi-solid electrolyte for DSC devices. Especially for the preparation of quasi-solid electrolytes where colloidal suspensions of solids in a proper solvent is used, the morphology and particle size of suspended materials is of fundamental importance. To this purpose, nanosized LDH was prepared by properly modifying the urea method[17] and used as a matrix to intercalate the I_3^-/I^- redox couple.

Synthetic parameters as solvent, urea/Al(III) molar ratio, and reaction time were finely adapted. In order to inhibit the crystal growth, the reaction time was shortened to six hours, and a mixture of water and ethylene glycol (1:2 v/v) was used as a solvent. The choice of the solvent mixture was made on the basis of literature data.[20] By using these conditions, we found that decreasing the urea/Al(III) molar ratio to 4 made it possible to prepare LDH in anionic forms different from carbonate, depending on the metal salts used for the synthesis. In this case, LDH in chloride form was precipitated from a solution containing zinc and aluminum chlorides. The compound had the following formula: $[Zn_{0.74}Al_{0.26}(OH)_2](Cl)_{0.26}\cdot 0.5H_2O$ (n-ZnAl-Cl). In our opinion, the possibility to obtain LDH compounds in anionic form different from carbonate directly from the synthesis is a relevant aspect that deserves further attention and will be discussed elsewhere.

In order to avoid particle aggregations, the sample was washed with CO_2-free distilled water and stored as colloidal dispersion in the same solvent used for the synthesis. The n-ZnAl-Cl size was investigated by TEM, and a micrograph of the LDH, reported in Figure 9, shows that the colloidal dispersion is made of hexagonal platelets having diameter of about 40−50 nm.

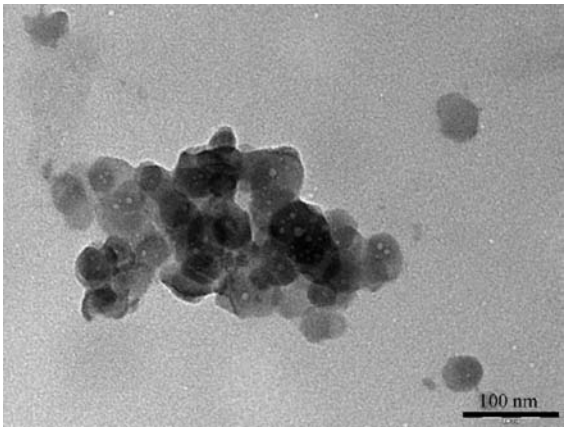

Figure 9. TEM micrograph of n-ZnAl-Cl.

After I^- exchange, the compound with formula $[Zn_{0.74}Al_{0.26}(OH)_2](Cl)_{0.08}I_{0.18}\cdot 0.43H_2O$ (n-ZnAl-I) was obtained. In Figure 10 the XRPD patterns of wet n-ZnAl

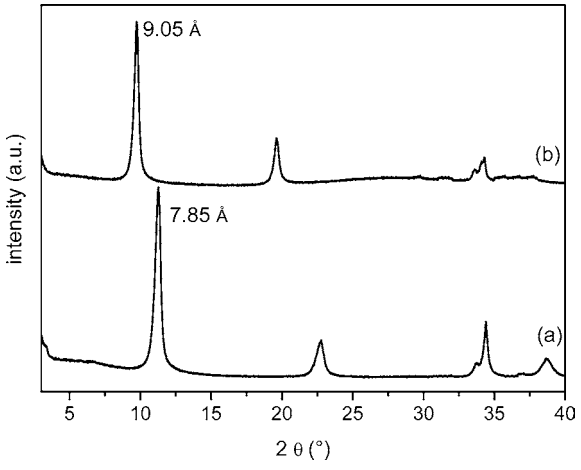

Figure 10. XRPD pattern of wet n-ZnAl-Cl (a), n-ZnAl-I (b).

containing chloride and iodide anions are compared. The n-ZnAl-I interlayer distance reaches the value of 9.05 Å, attributable to a highly hydrated n-ZnAl-I.

Taking into account the results obtained with the micrometric LDH (vide supra), the immobilization of triiodide

dx.doi.org/10.1021/ic202520v | Inorg. Chem. 2012, 51, 2560−2568

species on LDH has been performed using a 0.5 M I_2 solution in acetonitrile. The n-ZnAl-I_2 sample obtained had formula $[Zn_{0.74}Al_{0.26}(OH)_2](Cl)_{0.08}I_{0.18}(I_2)_{0.11}\cdot 0.57H_2O$ with 61.1% of loaded iodine. Figure 11 shows the XRPD pattern of the

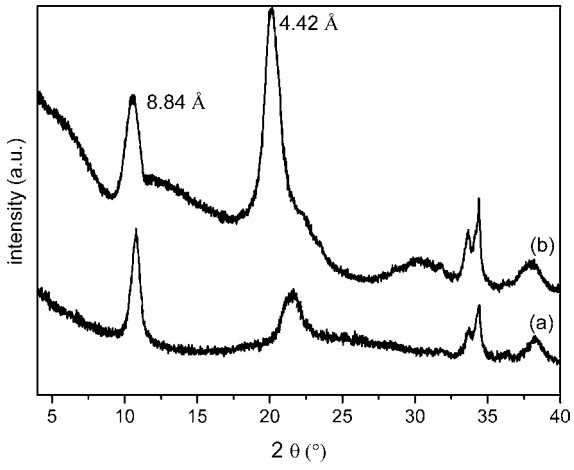

Figure 11. XRPD patterns of n-ZnAl-I (a) and n-ZnAl-I_2 (b) dried at room temperature.

recovered brown solid compared with the pristine n-ZnAl-I. The simulated XRPD patterns of LDH phases having composition similar to those experimentally observed for n-ZnAl-I and n-ZnAl-I_2 finely describe the experimental trends (Figure 12). In this case, different from the micrometric LDH,

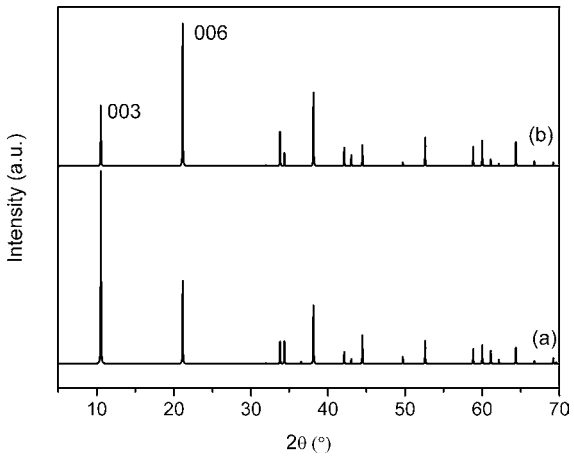

Figure 12. Simulated XRPD pattern of $[Zn_{0.74}Al_{0.26}(OH)_2](Cl)_{0.08}I_{0.18}\cdot 0.43H_2O$ (a) and $[Zn_{0.74}Al_{0.26}(OH)_2](Cl)_{0.08}I_{0.18}(I_2)_{0.11}\cdot 0.57H_2O$ (b).

the lower molar fraction of aluminum and then the lower ion exchange capacity generates an interlayer region with a lower content of iodide and triiodide. For the n-ZnAl-I_2 sample (Figure 12b), the electron density of 003 metal hydroxide planes is slightly larger than that of 006 interlayer planes; as a consequence, the intensity of the former diffraction peak is reduced. Moreover, the XRPD pattern of n-ZnAl-I_2 (Figure 11) shows a reflection at 8.84 Å attributable to 003 planes of the intercalated triiodide.

The TEM images of the n-ZnAl-I_2 sample (Figure 13) show aggregates of particles with diameter of about 40−50 nm, but some larger particles with diameter of about 300 nm are present. Arrows in Figure 13 indicate that some plates are

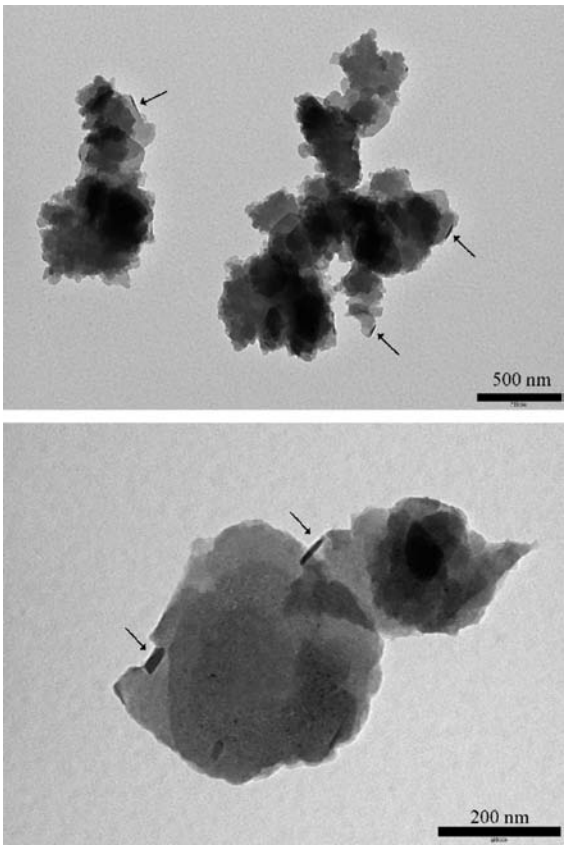

Figure 13. TEM micrographs of n-ZnAl-I_2.

starting to roll. Several authors proposed that the rolling of these lamellar structures arises from a reduction of the interactions between neighboring layers and interlayer anions, which makes the layered structure unstable at the foreland of hexagonal sheets. In order to maintain the charge balance, the brucite sheets are forced to close onto themselves.[33] This indicates that the material undergoes a partial exfoliation when intercalated with triiodide anions. The presence of a large amount of weakly held species breaks the network of hydrogen bonds, which prevents the LDH exfoliation, allowing the solvent to diffuse between the layers.[34]

The DR-UV−vis spectrum of the n-ZnAl-I_2 sample (see Figure S3 in the Supporting Information) is characterized by the presence absorptions typical of both I^- and I_3^- species, together with an additional amount of I_2 and polyiodide species. These data indicated that the intercalation procedure optimized for micrometric LDH samples is effective for the introduction of I_3^-/I^- species in nanosized LDH samples.

■ CONCLUSIONS

LDH materials containing the triiodide/iodide redox couple were obtained via intercalation of molecular iodine from nonaqueous solution in ZnAl-I. The molecular iodine is able to diffuse into the interlayer region of the LDH and to combine with the iodide forming triiodide and polyiodide, as shown by UV−vis spectra, collected on the dark brown colored products. The iodine/iodide molar ratio in the solids was affected by both I_2 concentration and solvent nature of the equilibrating solution. First, the increase of the I_2 concentration led to an increase in the amount of intercalated iodine in all solvents used. Second, the stability of adducts that iodine form with n-

dx.doi.org/10.1021/ic202520v | Inorg. Chem. 2012, 51, 2560−2568

donor solvents determined the amount of the intercalated iodine. It was interesting to find that the iodine loading increases as electron donor strength of the solvent decreases (diethyl ether > acetonitrile > ethanol ≫ chloroform). An anomalous behavior was observed in acetonitrile, a good coordinating and very polar solvent, where the iodine uptake reached 81.8%. In this case we have hypothesized that the intercalation process can also occur with an alternative ion exchange mechanism, thanks to the formation of triiodide anions in solution. The intercalation of iodine from acetonitrile was extended to well dispersible LDH having nanometric dimensions, synthesized modifying the urea method used for the preparation of micrometric LDH.

The intercalation of neutral inorganic molecules by LDH is a rather rare phenomenon that deserves attention to develop new materials with peculiar properties.

This paper has shown that LDH can be obtained with controlled dimensions and easily functionalized by intercalating large amounts of the I_3^-/I^- redox couple and therefore can be useful for application in quasi-solid electrolyte DSC devices. Furthermore the presence of polyiodide could favor the Grotthuss mechanism of electron transfer and improve DSC performances.

■ ASSOCIATED CONTENT

Supporting Information

Atomic coordinates and thermal displacement parameters, bond distances and angles, composition of samples, SEM micrographs, FT-IR spectra, and UV−vis spectra. This material is available free of charge via the Internet at http://pubs.acs.org.

■ AUTHOR INFORMATION

Corresponding Author

*E-mail: nocchett@unipg.it.

Notes

The authors declare no competing financial interest.

■ REFERENCES

(1) (a) Grätzel, M. *J. Photochem. Photobiol.* **2004**, *164*, 3. (b) Desilvestro, J.; Grätzel, M.; Kavan, L.; Moser, J. E.; Augustynski, J. *J. Am. Chem. Soc.* **1985**, *107*, 2988. (c) Vlachopoulos, N.; Liska, P.; Augustynski, J.; Grätzel, M. *J. Am. Chem. Soc.* **1988**, *110*, 1216. (d) O'Regan, B.; Grätzel, M. *Nature* **1991**, *335*, 737. (e) Nazeeruddin, M. K.; Kay, A.; Rodicio, I.; Humphrey-Baker, R.; Müller, E.; Liska, P.; Vlachopoulos, N.; Grätzel, M. *J. Am. Chem. Soc.* **1993**, *115*, 6382. (f) Grätzel, M. *Nature* **2001**, *414*, 338.

(2) Katakabe, T.; Kawano, R.; Watanabe, M. *Solid State Lett.* **2007**, *10*, F23.

(3) (a) Bach, U.; Lupo, D.; Comte, P.; Moser, J. E.; Weissortel, F.; Salbeck, J.; Spreitzer, H.; Gratzel, M. *Nature* **1998**, *395*, 583. (b) Kitamura, T.; Maitani, M.; Matsuda, M.; Wuda, Y.; Yanagida, S. *Chem. Lett.* **2001**, 1054.

(4) (a) Wang, H. X.; Xue, B. F.; Hu, Y. S.; Wang, Z. X.; Meng, Q. B.; Huang, X. J.; Chen, L. Q. *Electrochem. Solid State Lett.* **2004**, *7*, A302. (b) Stergiopoulos, T.; Arabatzis, I. M.; Katsaros, G.; Falaras, P. *Nano Lett.* **2002**, *2*, 1259.

(5) Li, D.; Qin, D.; Deng, M.; Luo, Y.; Meng, Q. *Energy Environ. Sci.* **2009**, *2*, 283.

(6) Wang, H. X.; Li, H.; Xue, B. F.; Wang, Z. X.; Meng, Q. B.; Chen, L. Q. *J. Am. Chem. Soc.* **2005**, *127*, 6394.

(7) (a) Park, J. H.; Kim, B.-W.; Moon, J. H. *Electrochem. Solid State Lett.* **2008**, *11*, B171. (b) Tsui, M.-C.; Tung, Y.-L.; Tsai, S.-Y.; Lan, C.-W. *J. Sol. Energy Eng.* **2011**, *133*, 011002.

(8) Wang, P.; Zakeeruddin, S. M.; Moser, J. E.; Nazeeruddin, M. K.; Sekiguchi, T.; Grätzel, M. *Nat. Mater.* **2003**, *2*, 402.

(9) (a) Trifirò, F.; Vaccari, A.; Cavani, F. *Catal. Today* **1991**, *11*, 173. (b) Rives, V. In *Layered Double Hydroxides: Present and Future*; Rives, V., Ed.; Nova Science Publishers: New York, 2001. (c) Jones, W.; Newman, S. P. *New J. Chem.* **1998**, *22*, 105. (d) Khan, A. I.; O'Hare, D. *J. Mater. Chem.* **2002**, *12*, 1. (e) Leroux, F.; Taviot-Guého, C. *J. Mater. Chem.* **2005**, *15*, 3628. (f) Braterman, P. S.; Xu, Z. P.; Yarberry, F. In *Handbook of Layered Materials*; Auerbach, S. M., Carrado, K. A., Dutta, P. K., Eds; Marcel Dekker: New York, 2004; p 373. (g) Oh, J.-M.; Biswick, T. T.; Choy, J.-H. *J. Mater. Chem.* **2009**, *19*, 2553. (h) Li, F.; Duan, X. *Applications of Layered Double Hydroxides in Structure and Bonding*; Springer-Verlag: Berlin, 2006; Vol. *119*, p 193.

(10) (a) Costantino, U.; Gallipoli, A.; Nocchetti, M.; Camino, G.; Bellucci, F.; Frache, A. *Polym. Degrad. Stab.* **2005**, *90*, 586. (b) Costantino, U.; Montanari, F.; Nocchetti, M.; Canepa, F.; Frache, A. *J. Mater. Chem.* **2007**, *17*, 1079. (c) Costa, F. R.; Saphiannikova, M.; Wagenknecht, U.; Heinrich, G. *Adv. Polym. Sci.* **2008**, *210*, 101. (d) Aloisi, G. G.; Elisei, F.; Nocchetti, M.; Camino, G.; Frache, A.; Costantino, U.; Latterini, L. *Mater. Chem. Phys.* **2010**, *123*, 372. (e) Costantino, U.; Nocchetti, M.; Sisani, M.; Vivani, R. *Z. Kristallogr.* **2009**, *224*, 273. (f) Costantino, U.; Bugatti, V.; Gorrasi, G.; Montanari, F.; Nocchetti, M.; Tammaro, L.; Vittoria, V. *ACS Appl. Mater. Interfaces* **2009**, *1*, 668. (g) Costantino, U.; Nocchetti, M.; Tammaro, L.; Gorrasi, G. In *Multifunctional and Nanoreinforced Polymers for Food Packaging*; Lagaron, J. M., Ed.; Woodhead Publishing: Cambridge, 2011; Chapter 3, p 43. (h) Evans, D. G.; Duan, X. *Chem. Commun.* **2006**, 485.

(11) (a) Vaccari, A. *Appl. Clay Sci.* **1999**, *14*, 161. (b) Turco, M.; Bagnasco, G.; Costantino, U.; Marmottini, F.; Montanari, T.; Ramis, G.; Busca, G. *J. Catal.* **2004**, *228*, 43. (c) Montanari, T.; Sisani, M.; Nocchetti, M.; Vivani, R.; Concepcion Herrera Delgado, M.; Ramis, G.; Busca, G.; Costantino, U. *Catal. Today* **2010**, *152*, 104. (d) Busca, G.; Costantino, U.; Montanari, T.; Ramis, G.; Resini, C.; Sisani, M. *Int. J. Hydrogen Energy* **2010**, *35*, 5356.

(12) (a) Latterini, L.; Nocchetti, M.; Costantino, U.; Aloisi, G. G.; Elisei, F. *Inorg. Chim. Acta* **2007**, *360*, 728. (b) Latterini, L.; Nocchetti, M.; Aloisi, G. G.; Costantino, U.; De Schryver, F.; Elisei, F. *Langmuir* **2007**, *23*, 12337. (c) Shi, W.; Wei, M.; Lu, J.; Evans, D. G.; Duan, X. *J. Phys. Chem. C* **2009**, *113*, 12888.

(13) (a) Gomes Silva, C.; Bouizi, Y.; Fornes, V.; Garcia, H. *J. Am. Chem. Soc.* **2009**, *131*, 13833. (b) Meng, W.; Li, F.; Evans, D. G.; Duan, X. *J. Porous Mater.* **2004**, *11*, 97. (c) Shao, M.; Han, J.; Wei, M.; Evans, D. G.; Duan, X. *Chem. Eng. J.* **2011**, *168*, 519.

(14) (a) Ma, R.; Liu, Z.; Li, L.; Iyi, N.; Sasaki, T. *J. Mater. Chem.* **2006**, *16*, 3809. (b) Gardner, E.; Huntoon, K. M.; Pinnavaia, T. J. *Adv. Mater.* **2001**, *13*, 1263. (c) Woo, M. A; Song, M.-S.; Woo Kim, T.; Kim, I. Y.; Ju, J.-Y.; Lee, Y. S.; Kim, S. J.; Choy, J.-H.; Hwang, S.-J. *J. Mater. Chem.* **2011**, *21*, 4286.

(15) (a) Bendall, J. S.; Paderi, M.; Ghigliotti, F.; Li Pira, N.; Lambertini, V.; Lesnyak, V.; Gaponik, N.; Visimberga, G.; Eychmüller, A.; Sotomayor Torres, C. M.; Welland, M. E.; Gieck, C.; Marchese, L. *Adv. Funct. Mater.* **2010**, *20*, 3298. (b) Yan, D.; Lu, J.; Wei, M.; Qin, S.; Chen, L.; Zhang, S.; Evans, D. G.; Duan, X. *Adv. Funct. Mater.* **2011**, *21*, 2497.

(16) Kopka, H.; Beneke, K.; Lagaly, G. *J. Colloid Interface Sci.* **1988**, *123*, 427.

(17) Costantino, U.; Marmottini, F.; Nocchetti, M.; Vivani, R. *Eur. J. Inorg. Chem.* **1998**, 1439.

(18) (a) Israeli, Y.; Taviot-Guelo, C.; Besse, J. P.; Morel, J. P. *J. Chem. Soc., Dalton Trans.* **2000**, 791. (b) Bontchev, R. P.; Liu, S.; Krumhansl, J. L.; Voigt, J.; Nenoff, T. M. *Chem. Mater.* **2003**, *15*, 3669. (c) Prasanna, S. V.; Kamat, P. V.; Shivakumara, C. *J. Colloid Interface Sci.* **2010**, *344*, 508. (d) Iyi, N.; Fujii, K.; Okamoto, K.; Sasaki, T. *Appl. Clay Sci.* **2007**, *35*, 218. (e) Allada, R. K.; Pless, J. D.; Nenoff, T. M.; Navrotsky, A. *Chem. Mater.* **2005**, *17*, 2455.

(19) Mohanambe, L.; Vasudevan, S. *Inorg. Chem.* **2004**, *43*, 6421.

(20) Ma, R.; Liang, J.; Takada, K.; Sasaki, T. *J. Am. Chem. Soc.* **2011**, *133*, 613.

(21) Adachi-Pagano, M.; Forano, C.; Besse, J. P. *J. Mater. Chem.* **2003**, *13*, 1988.

(22) Larson, C.; von Dreele, R. B. *Generalized Crystal Structure Analysis System*; Los Alamos National Laboratory: Los Alamos, NM, 2001.
(23) (a) Prevot, V.; Forano, C.; Besse, J. P. *J. Mater. Chem.* **1999**, *9*, 155. (b) Prasanna, S. V.; Vishnu Kamath, P.; Shivakumara, C. *J. Colloid Interface Sci.* **2010**, *344*, 508.
(24) Svensson, H.; Kloo, L. *Chem. Rev.* **2003**, *103*, 1649.
(25) Kraus, W.; Nolze, G. *J. Appl. Crystallogr.* **1996**, *29*, 301.
(26) (a) Chapman, K. W.; Chupas, P. J.; Nenoff, T. M. *J. Am. Chem. Soc.* **2010**, *132*, 8897. (b) Sava, D. F.; Rodriguez, M. A.; Chapman, K. W.; Chupas, P. J.; Greathouse, J. A.; Crozier, P. S.; Nenoff, T. M. *J. Am. Chem. Soc.* **2011**, *133*, 12398. (c) Chapman, K. W.; Sava, D. F.; Chupas, P. J.; Halder, G. J.; Nenoff, T. M. *J. Am. Chem. Soc.* **2011**, *133*, 18583.
(27) (a) Greenwood, N. N.; Earnshaw, A. *In Chemistry of the Elements*; Pergamon Press Ltd.: Oxford, 1984. (b) Maguire, J. A.; Banewicz, J. J.; Hung, R. C. T.; Wright, K. L. *Inorg. Chem.* **1972**, *11*, 3059.
(28) (a) Kimura, K.; Achiba, Y.; Katsumata, S. *J. Phys. Chem.* **1973**, *77*, 2520. (b) Tse, H. C.; Tamres, M. *J. Phys. Chem.* **1977**, *81*, 1367. (c) Tamres, M.; Brandon, M. *J. Am. Chem. Soc.* **1960**, *82*, 2134.
(29) (a) Popov, A.; Geske, D. *J. Am. Chem. Soc.* **1957**, *80*, 1340. (b) Popov, A.; Deskin, W. A. *J. Am. Chem. Soc.* **1958**, *80*, 2976.
(30) Miyata, S. *Solid State Ionics* **1983**, *22*, 135.
(31) (a) Gabes, W.; Stufkens, D. J. *Spectrochim. Acta, Part A* **1974**, *30A*, 1835. (b) Antoniadis, C. D.; Hadjikakou, S. K.; Hadjiliadis, N.; Kubicki, M.; Butler, I. S. *Eur. J. Inorg. Chem.* **2004**, *21*, 4324.
(32) Hasel, T.; Schmidtmann, M.; Cooper, A. I. *J. Am. Chem. Soc.* **2011**, *133*, 14920.
(33) (a) Ren, L.; Hu, J. S.; Wan, L. J.; Bai, C. L. *Mater. Res. Bull.* **2007**, *42*, 571. (b) Wang, X.; Zhuang, J.; Chen, J.; Zhou, K.; Li, Y. *Angew. Chem.* **2004**, *116*, 2051. (c) Liu, X.; Ma, R.; Bando, Y.; Sasaki, T. *Angew. Chem., Int. Ed.* **2010**, *49*, 8253.
(34) Ma, R.; Liu, Z.; Li, L.; Iyi, N.; Sasaki, T. *J. Mater. Chem.* **2006**, *16*, 3809.